

Predictive Reactor Pressure Vessel Steel Irradiation Embrittlement Models: Issues and Opportunities

G.R. Odette and R.K. Nanstad

Nuclear plant life extension to 80 years will require accurate predictions of neutron irradiation-induced increases in the ductile-brittle transition temperature (ΔT) of reactor pressure vessel steels at high fluence conditions that are far outside the existing database. Remarkable progress in mechanistic understanding of irradiation embrittlement has led to physically motivated ΔT correlation models that provide excellent statistical fits to the existing surveillance database. However, an important challenge is developing advanced embrittlement models for low flux-high fluence conditions pertinent to extended life. These new models must also provide better treatment of key variables and variable combinations and account for possible delayed formation of "late blooming phases" in low copper steels. Other issues include uncertainties in the compositions of actual vessel steels, methods to predict ΔT attenuation away from the reactor core, verification of the master curve method to directly measure the fracture toughness with small specimens and predicting ΔT for vessel annealing re-mediation and re-irradiation cycles.

INTRODUCTION

Neutron irradiation can cause severe embrittlement in reactor pressure vessel (RPV) steels.^{1,2} While specific in application, the topic of RPV embrittlement covers a very diverse range of activities, ranging from fundamental multiscale modeling and nanofeature characterization studies to fracture mechanics assessments of vessel integrity, that are far too broad to cover in this brief review. Thus, we will more narrowly focus here on current U.S. regulatory approaches to predicting embrittlement in order to provide a coherent

How would you...

...describe the overall significance of this paper?

Demonstrating that massive pressure vessels maintain large safety margins against fast fracture will be required to extend nuclear reactor plant operation to 80 years in the face of irradiation embrittlement. Unfortunately, there is no embrittlement database for 80-year vessel conditions. Notably, current regulatory models both under-predict embrittlement measured in accelerated tests, and do not reflect new damage processes that may emerge during extended life. Thus, advanced, physically based, and empirically verified embrittlement models are needed.

...describe this work to a materials science and engineering professional with no experience in your technical specialty?

Neutron irradiation can cause severe elevation of the brittle fracture temperatures in steels due to precipitation and defect hardening. Unfortunately, there is almost no data for high dose, extended life conditions and results from accelerated tests are not reliable due to the complex effects of dose rates. High doses may also produce additional hardening features like "late-blooming phases." Research to develop models of precipitation and defect accumulation, needed to predict embrittlement for extended life, is described.

...describe this work to a layperson?

Nuclear plant life extension to 80 years will provide a significant carbon-free energy resource. Massive reactor pressure vessels are the first line of defense against release of radiation. Thus, life extension will require proof, beyond almost any shadow of a doubt, that the vessel will not fracture under any conceivable circumstance by assuring that the effects of long-term irradiation on the fracture toughness do not significantly degrade large inherent safety margins.

framework for discussion. Regulations currently characterize the most critical form of embrittlement in terms of elevation of the temperature regime of brittle cleavage fracture, characterized by Charpy V-notch impact test 41J temperature shifts (ΔT), as illustrated in Figure 1a.³

The U.S. Regulatory Guide 1.99, Revision 2 (RG 1.99-2) provides the current generic basis to evaluate ΔT in terms of the copper and nickel contents of a steel and fast neutron fluence ($E > 1$ MeV) for weld and plate product forms.⁴ The model equations for RG 1.99-2 were statistically fit to a small surveillance database (177 data points) on steels irradiated in surveillance capsules at flux levels somewhat higher (1 to slightly over 5) than at the vessel wall itself. The RG 1.99-2 model was derived prior to 1985 and reflects the then emerging, but far from complete, physical understanding of embrittlement mechanisms.⁵ A large body of higher flux test reactor data was not used in developing RG 1.99-2.

However, over the last 25 years tremendous advances in understanding embrittlement mechanisms, and improved physically motivated ΔT models, such as described in Reference 1, now provide generally excellent statistical fits to a much larger U.S. power reactor (surveillance) embrittlement database (PREDB). Further, the test reactor database has evolved, and now includes the results of the Irradiation Variables (IVAR) program.⁶ This program was a large systematic effort to characterize embrittlement mechanisms, to develop high-resolution maps of the effects of embrittlement variables and variable combinations, with special emphasis on flux effects, and to provide independent checks on the

PREDB-based ΔT models.

Since *RG 1.99-2* neither provides a good fit to the existing PREDB, nor reflects current understanding of embrittlement mechanisms, research has

continued to develop improved ΔT models, including one that has already been used in regulatory assessments of pressurized thermal shock.¹ In the following sections we will briefly review

the status of the recent ΔT models, with emphasis on the major outstanding issues. In summary:

- ΔT depends on combined effects of neutron flux (ϕ), flux spectrum, fluence (ϕt), irradiation temperature (T_i), alloy composition (Cu, Ni, Mn, P), and start-of-life microstructure, or product form.^{1,2,7} Due to scatter and clumped and confounded distributions of variables, however, the PREDB lacks the resolution to statistically identify a “best” ΔT model. Properly supplementing the PREDB with high-resolution IVAR and other qualified test reactor data will be needed to significantly improve the reliability of future ΔT models.
- Existing ΔT models cannot reliably extrapolate to high fluence levels of up to $\approx 10^{20}$ n/cm² pertinent to pressurized water reactor extended life conditions, since 99% of the PREDB data is at $< 5 \times 10^{19}$ n/cm². Thus, high fluence data from other surveillance programs and test reactor irradiations must be used to develop improved ΔT models for extended life. Figure 1b shows predicted minus measured residuals for a successful low flux PREDB based ΔT model¹ applied to a large independent body of higher flux test reactor data, compiled by M. EricksonKirk.⁸ (M. EricksonKirk provided test reactor database to the authors in the form of an *Excel* spreadsheet. EricksonKirk also derived a number of ΔT models based on systematic fits to the PREDB and selected subsets of the test reactor database, as described in detail in the draft NRC report *Technical Basis for Revision of Regulatory Guide 1.99: NRC Guidance on Methods to Estimate the Effects of Radiation Embrittlement on the Charpy V-Notch Impact Toughness of Reactor Vessel Materials*. A summary of this work is presented in Reference 8.) The large negative residuals that increase with fluence show that the model systematically and significantly underpredicts ΔT . Thus, reliably modeling high fluence embrittlement at the much

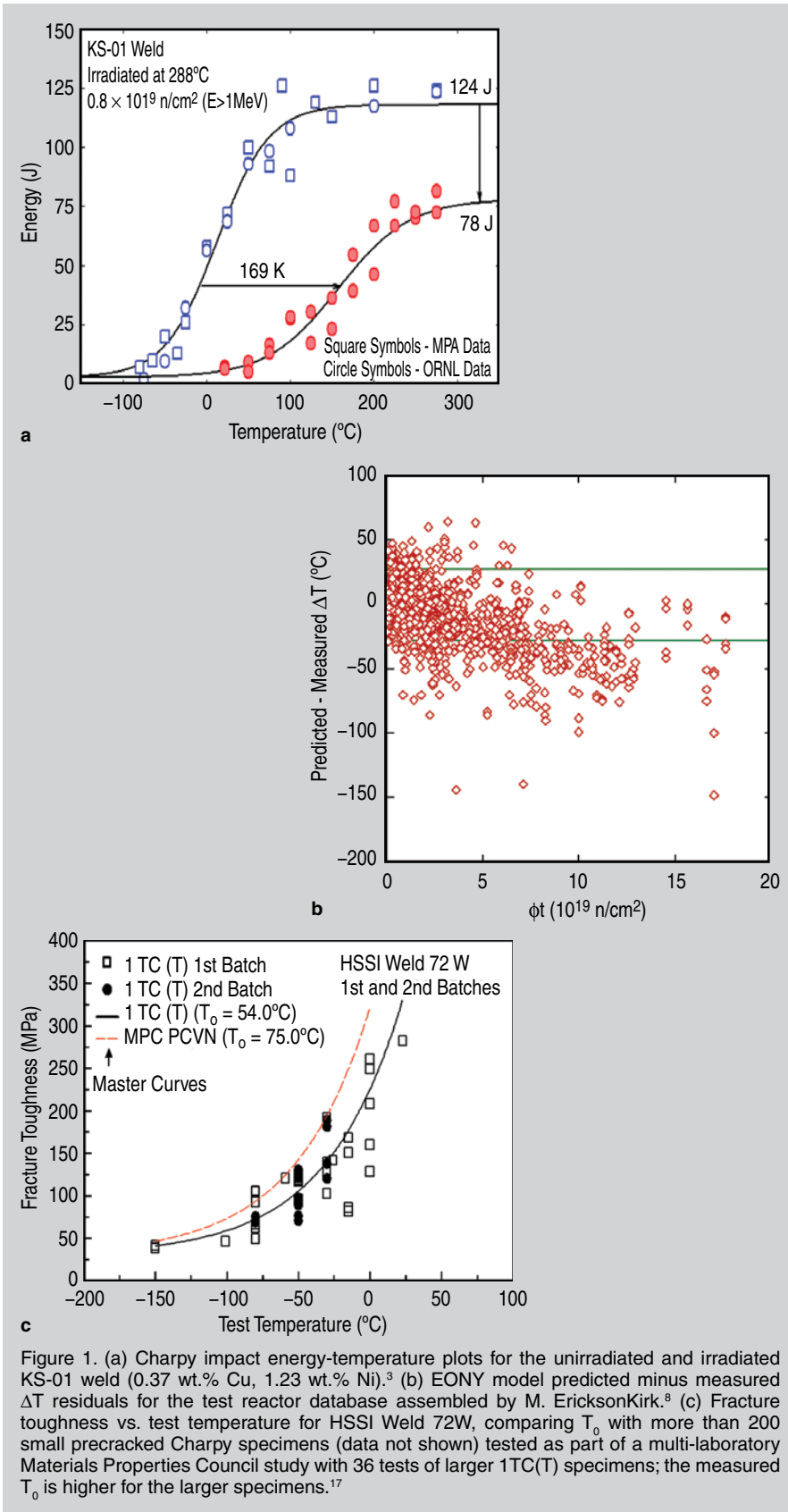


Figure 1. (a) Charpy impact energy-temperature plots for the unirradiated and irradiated KS-01 weld (0.37 wt.% Cu, 1.23 wt.% Ni).³ (b) EONY model predicted minus measured ΔT residuals for the test reactor database assembled by M. EricksonKirk.⁸ (c) Fracture toughness vs. test temperature for HSSI Weld 72W, comparing T_0 with more than 200 small precracked Charpy specimens (data not shown) tested as part of a multi-laboratory Materials Properties Council study with 36 tests of larger 1TC(T) specimens; the measured T_0 is higher for the larger specimens.¹⁷

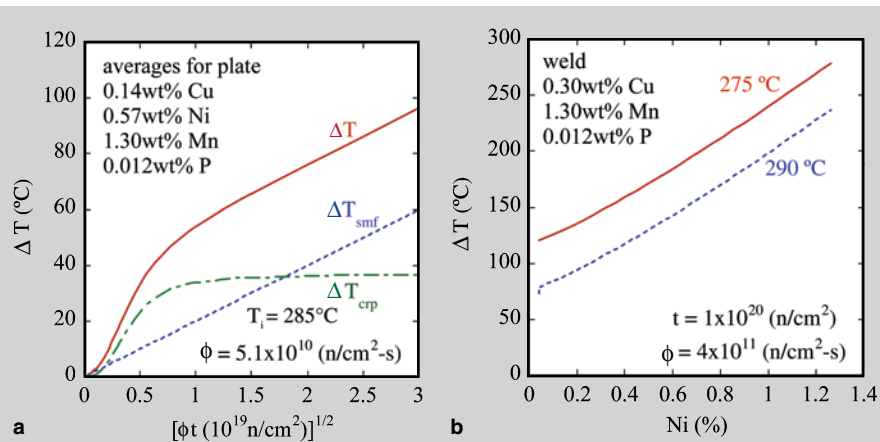


Figure 2. The EONY ΔT predictions:¹ (a) for plate at the average Cu, Ni, Mn, and P compositions and irradiation temperature and flux in the PREDB database; (b) the effect of nickel on ΔT for a 0.30 wt.% Cu weld at 10^{20} n/cm² and at two irradiation temperatures.

lower RPV fluxes is critical.

- Models have long predicted that Mn-Ni-Si late-blooming phases (LBPs) could form in low-copper steels after a significant incubation fluence (hence, the term “late blooming”), resulting in severe unanticipated ΔT .^{2,7,9-12} Current regulatory ΔT models do not reflect

potential LBP contributions to ΔT . However, recent research has clearly demonstrated the existence of LBPs for a wide range of alloys and irradiation conditions.¹²⁻¹⁵

Other issues that cannot be addressed here because of space limitations include the following items.

- The effects of neutron flux, flu-

ence, and spectrum, in combination with all the other embrittlement variables, on attenuation of embrittlement away from the reactor core are not well modeled. Further, the potential for long time at temperature thermal aging is not understood. Finally, the effects of very low flux boiling water reactor conditions on ΔT are not fully resolved.

- Annealing could be used to remediate severely embrittled vessels during extended life. However, the U.S. database on irradiation, annealing, and re-embrittlement is incomplete and almost entirely limited to test reactor data at relatively low fluence.
- The master curve method¹⁶ to evaluate toughness-temperature curve [$K_{Ic}(T-T_0)$] reference temperatures (T_0), as illustrated for a Linde 124 weld in Figure 1c,¹⁷ is a more accurate approach to vessel integrity assessment than current Charpy ΔT -based regulations.

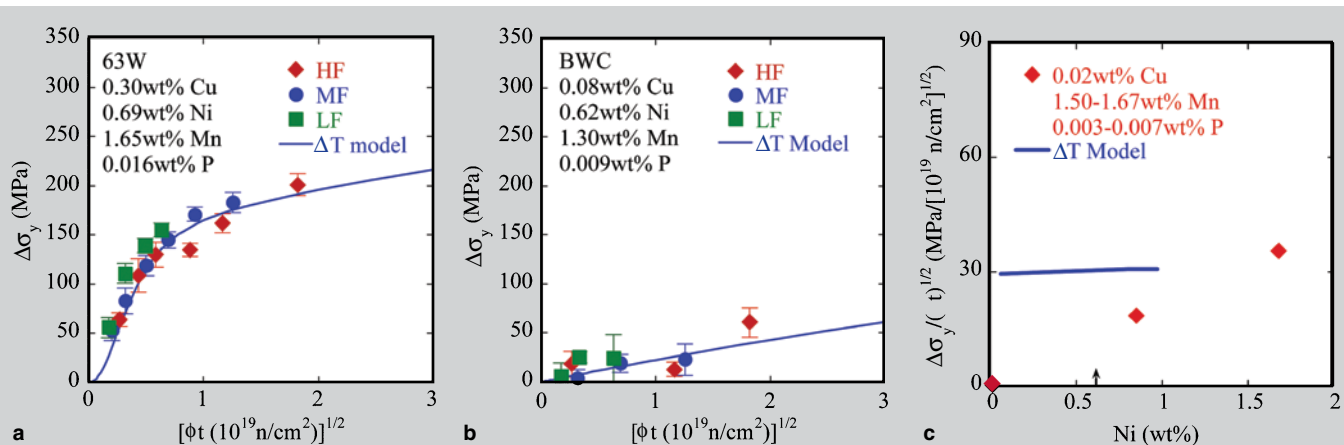


Figure 3. (a) and (b) EONY surveillance based predictions (solid lines) of $\Delta\sigma_y$ (converted) versus the square root of fluence compared to high (HF), medium (MF), and low flux (LF) IVAR data for a high copper (a) and low copper (b) welds;¹ (c) comparisons of the effect of nickel on SMF hardening in the IVAR data versus the EONY model predictions for plate.

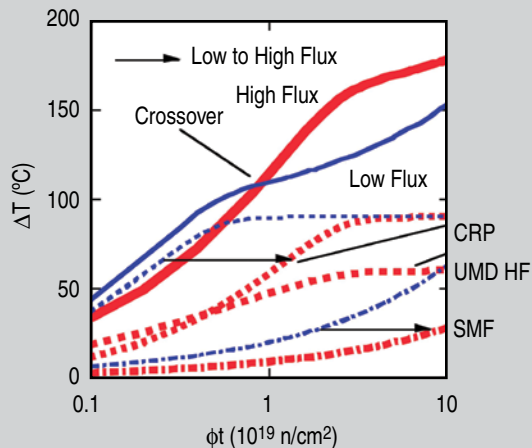


Figure 4. A schematic illustration of the three-feature (SMF + CRP + UMD) ΔT model for a copper-bearing steel. The heavy and light lines are for high and low flux, respectively. The arrows show the delays in the SMF and CRP contributions at high flux. The longer dashed line shows the extra UMD contribution to ΔT_{umd} at high flux. These competing effects result in a crossover in the total ΔT .

However, unresolved master curve issues include: small specimen constraint loss leading to non-conservative (negative) T_0 biases, as illustrated in the comparison of precracked Charpy specimens and larger compact tension specimens shown in Figure 1c;¹⁷ the validity and physical basis for a universal $K_{Ic}(T-T_0)$ master curve shape; and the applicability of the method to vessel flaws and conditions other than cleavage initiation.

More generally, applying any integrity assessment method with smaller safety margins than used in current practice based on testing surrogate materials that may not be the same as in the actual vessel, raises significant issues.

PREDB-BASED ΔT MODELS—STATUS AND OPPORTUNITIES

Embrittlement is primarily due to irradiation hardening ($\Delta\sigma_y$) caused by ultra-high number densities of nanometer-scale dislocation obstacles hardening features that form as the result of point defect and solute clustering, accelerated by radiation enhanced diffusion.^{1,2,7,10} At low flux, and low to intermediate nickel, hardening and embrittlement are primarily due to persistent defect-solute cluster stable matrix features (SMFs) and, in copper-bearing steels ($> \approx 0.07$ wt.%), copper-rich precipitates (CRPs). Thus, embrittlement models are typically cast in the form $\Delta T = \Delta T_{smf} + \Delta T_{cp}$, where the ΔT_{smf} and ΔT_{cp} fitting equations are physically motivated functions of the key irradiation and metallurgical variables. Eason, Odette, Nanstad, and Yamamoto (EONY)¹ recently developed a ΔT model fit to the PREDB (829 data points) using physically motivated functions of ϕ , ϕt , T_i , Cu, Ni, P, Mn, and weld, plate, and forging product form. The EONY model has an average standard error $\approx 11.7^\circ\text{C}$. Figure 2a shows EONY ΔT predictions for an “average” PREDB plate irradiation as a function of the square root of fluence. The ΔT are modest ($< 100^\circ\text{C}$) in this case. Figure 2b shows a corresponding ΔT for a 0.3 wt.% copper weld as a function of nickel extrapolated to 10^{20} n/cm². The ΔT are very large at high

nickel, especially at lower irradiation temperature. Alternate models, differing in both the form of the functions and the fitting variables, can also yield similar statistical fits, while extrapolating to different ΔT predictions outside the PREDB. The EONY analysis dealt with this issue of the non-uniqueness in three primary ways:¹ using mechanistic understanding and broadly observed data trends to guide the selection of fitting functions and variables (see Chapter 2 of Reference 1); detailed analysis of residuals for all potential embrittlement variables; and direct comparisons of the model predictions to the independent IVAR database (see Chapter 6 of Reference 1).

Figure 3a and b compares EONY model predictions (with ΔT empirically converted to $\Delta\sigma_y$) to IVAR data for high and low copper surveillance welds, respectively. The good agreement observed in these examples is representative of similar comparisons for the overall IVAR database.¹ The IVAR data also show a systematic and significant flux effect, with an overall increase in $\Delta\sigma_y$ of about 40% for decreases of flux from $\approx 10^{12}$ to 8×10^{10} n/cm²-s.¹⁸ The EONY ΔT_{smf} and ΔT_{cp} models also predict a similar dependence on flux below $\approx 4 \times 10^{10}$ n/cm²-s, but the PREDB fits are unable to resolve this effect at higher flux. Figure 3c shows another example of the higher resolution power of the IVAR database, in this case for the effect of nickel on the SMF hardening (based on a fit to the low copper $\Delta\sigma_{smf}/\sqrt{(\phi t)}$ database). The EONY model is essentially independent of nickel, while a strong and systematic nickel effect is observed in the controlled IVAR single variable data. Other examples of the ability of the IVAR database to better resolve the effects of embrittlement variables include manganese effects on CRP hardening and the temperature dependence of both the SMF and CRP contributions.¹

These results lead to two important conclusions. First, the independent verification provided by the IVAR database demonstrates the broad validity of the EONY (and other similar) ΔT models. Second, the ΔT models can be refined by properly integrating the PREDB, IVAR, and other pertinent databases.

EMBRITTEMENT AT LOW FLUX AND HIGH FLUENCE

Figure 1b casts serious doubt on the ability of PREDB-based models to predict ΔT at high 80-year fluence up to $\approx 10^{20}$ n/cm², far beyond the current surveillance database. Fortunately, higher flux, accelerated test reactor irradiations can access this regime. However, flux influences the various hardening features and corresponding ΔT for a given alloy, irradiation temperature and fluence.^{18–20} Indeed, there is evidence that a significant population of a third defect that is thermally unstable under irradiation is important at high flux.^{19,20} Assuming that such unstable matrix defects (UMDs) are generated at a rate $\phi\sigma_{umd}$, while annealing under irradiation at a rate N_{umd}/τ_{umd} , it can be shown that at steady state $N_{umd} = \phi\sigma_{umd}\tau_{umd}$. Here, σ_{umd} , N_{umd} , and τ_{umd} are the UMD neutron formation cross section, number density, and annealing time, respectively, At fluxes less than $\approx 10^{12}$ n/cm²-s, the UMD concentrations, and corresponding ΔT contributions, are minimal. Increases from low to intermediate flux in this regime systematically delay the SMF and CRP ΔT contributions due to a solute trap vacancy–self interstitial atom recombination mechanism, which decreases the efficiency of radiation enhanced diffusion.¹⁸ At higher flux, however, larger concentrations of UMD play two competing roles.^{19,20} The UMD directly contribute to hardening and ΔT , but they also act as point defect sinks that delay the SMD and CRP ΔT contributions by further decreasing the efficiency of radiation enhanced diffusion.

As a result of this dual role of UMDs, higher flux can increase, decrease, or leave unaffected the ΔT , depending on the combination of all other embrittlement variables. Figure 4 schematically illustrates these three-feature model concepts. The arrows highlight the high flux UMD-induced delays in the CRP and SMF contributions, while the extra UMD contribution to hardening is shown by the dashed line. If there is a sufficiently large CRP contribution, the net effect is a cross-over in the $\Delta T(\phi t)$ curves: high flux decreases ΔT at low fluence and increases ΔT at high fluence. If the CRP contributions

are small, there is no crossover and high flux increases ΔT at all fluences.

A three feature model was developed based on these concepts about 15 years ago as part of research on the effects of flux on the balance of UMD, SMF, and CRP hardening contributions based on their respective annealing signatures^{19,20} The UMD recover quickly at low annealing temperatures ($<350^{\circ}\text{C}$) while SMF and CRP persist. These studies showed that low temperature annealing produces much more hardness recovery following high versus low flux irradiations, consistent with the corresponding variation in UMD concentrations. A modified version of the three-feature model was recently applied to analyze ΔT data from high flux test reactor irradiations that are under predicted at high fluence (see Figure 1b) by low flux PREDB (e.g., EONY) based models.^{1,21} This analysis suggested that these under predictions are due in part to the UMD flux effect that does not occur at low fluxes.

An example of the predictions of more recent elaboration of the three-feature model is shown in Figure 5. In this case, the EONY model was used to predict the SMF and CRP ΔT using an effective fluence ($\phi t_e > \phi t$) to account for the delays in the contributions of these features due to the effects of both UMD sinks and recombination on reducing the efficiency of radiation-enhanced diffusion. Figure 5a shows the raw ΔT (equivalent) data from higher flux BR-2 reactor RAMADO and lower flux IVAR irradiations of a 0.3 wt.% copper weld (73W). The delay in embrittlement in the high-flux Radamo data is clearly evident. Figure 5b compares the predictions of the three-feature model (solid line) with the data, adjusted by the model to a common high flux (5×10^{13} n/cm²-s) and 290°C irradiation condition. The dashed line shows there is a significant UMD ΔT_{umd} contribution at high flux. Figure 5c shows the corresponding plot at a common low flux (5×10^{10} n/cm²-s), with a negligible UMD contribution. Figure 5d shows the crossover of the high and low flux ΔT curves at intermediate fluence. Similar analysis of other alloys also generally shows good consistency between the three-feature model predictions and the adjusted test reactor data over a wide range of flux.

Thus, the three feature model at least partly rationalizes the under predictions shown by the residuals in Figure 1b. However, it must be emphasized that these preliminary results are by no means conclusive. For example, the nature of the UMDs in complex steels is not understood, and the UMD contributions appear to be larger than indicated in some other data sets.

Nevertheless, the preceding analysis supports the following tentative conclusions: some of the under predictions of the high fluence data, shown in Figure 1b, may be artifacts of high flux test reactor irradiation conditions; direct use of high flux test reactor data to predict ΔT for high fluence–low flux conditions may be inappropriate; basic experiments, such as low-temperature annealing, can be used to develop embrittlement models that account for a very wide range of flux; new high fluence test reactor irradiations are needed, and should be carried out at sufficiently low flux, so as to minimize the effects of UMDs; and, considerable research will be needed to verify, refine, and quantify three-feature, or alternative, models to predict ΔT at high fluence and low flux.

HIGH FLUENCE EMBRITTEMENT MECHANISMS

The strong effect of nickel on embrittlement (see Figure 2) has long been recognized, and the underlying mechanism was first modeled more than a decade ago.^{7,9–11} Thermodynamic models and microanalytical characterization studies have shown that strong Ni-Mn bonds and low Ni/Mn-Fe interface energies result in co-enrichment of these elements in nanometer-scale CRPs.^{7,9–15,22–31} This results in larger precipitate volume ($\text{Cu} + \text{Ni} + \text{Mn} > \text{Cu}$) and corresponding hardening. Lattice Monte Carlo simulations predicted precipitate structures with copper-rich cores surrounded by Mn-Ni rich shells,²⁶ which are observed in atom probe tomography (APT) studies.^{13,29} CRP enrichments are enhanced by higher alloy manganese and nickel levels, as well as by lower temperatures and copper contents.^{1,7,9–15,30,31} At higher enrichments ($>50\%$ Mn + Ni), CRPs give way to manganese- and nickel-rich precipitates (MNPs)

The typical range of manganese is modest (note, manganese is typically lower in forgings), while nickel contents vary from about 0.1 to 1.3 percent. Thus, the nickel effect has often been viewed in isolation, while in fact it derives from Ni-Mn synergisms. Similarly, Si-Ni and Si-Mn interactions also result in silicon enrichment in CRPs.

Thermodynamic-kinetic models also predicted the formation of Mn-Ni phases even in the absence of copper, but at low nucleation rates compared to that for CRPs, resulting in relatively high incubation fluences.^{7,9–12} However, as schematically illustrated in Figure 6a, once nucleated such late blooming Mn-Ni-Si phases (LBP) rapidly grow to large volume fractions, causing severe embrittlement. The models also show that small concentrations of copper may act as a catalyst for LBP nucleation. Notably, current TTS models do not reflect the potential LBP embrittlement contributions, probably in part, because they may require critical combinations of higher nickel and fluence and lower temperature and flux that have yet to be extensively encountered in the PREDB.

The IVAR irradiations contained both complex steels and simple ferritic model alloys that were specially designed to search for LBP and map their formation regimes. This search has clearly demonstrated the existence of LBP, as illustrated in Figure 6b, showing an APT map of manganese and nickel atom positions, and a blow-up view of an Mn-Ni precipitate, in a copper-free, 1.6Ni-1.6Mn wt.% model alloy. Similar observations are now reported by other researchers around the world.^{13–15} Figure 6c shows $\Delta\sigma_y$ for low copper steels and model ferritic alloys plotted as a function of the volume fraction of Mn-Ni(-Si) precipitates, measured by a resistivity-Seebeck coefficient technique.^{30,31} The arrow highlights two copper-free 1.6wt.% Ni-1.6wt.% Mn RPV steels (with different P contents), irradiated to 1.6×10^{19} n/cm² at 270°C and intermediate flux; the large precipitate volume fractions (f_p) and high $\Delta\sigma_y$, indicating that these alloy composition-irradiation conditions have clearly crossed the LBP boundary. Figure 6c also shows the $\Delta\sigma_y$ and precipitate volume fractions in steels with lower nickel contents and/

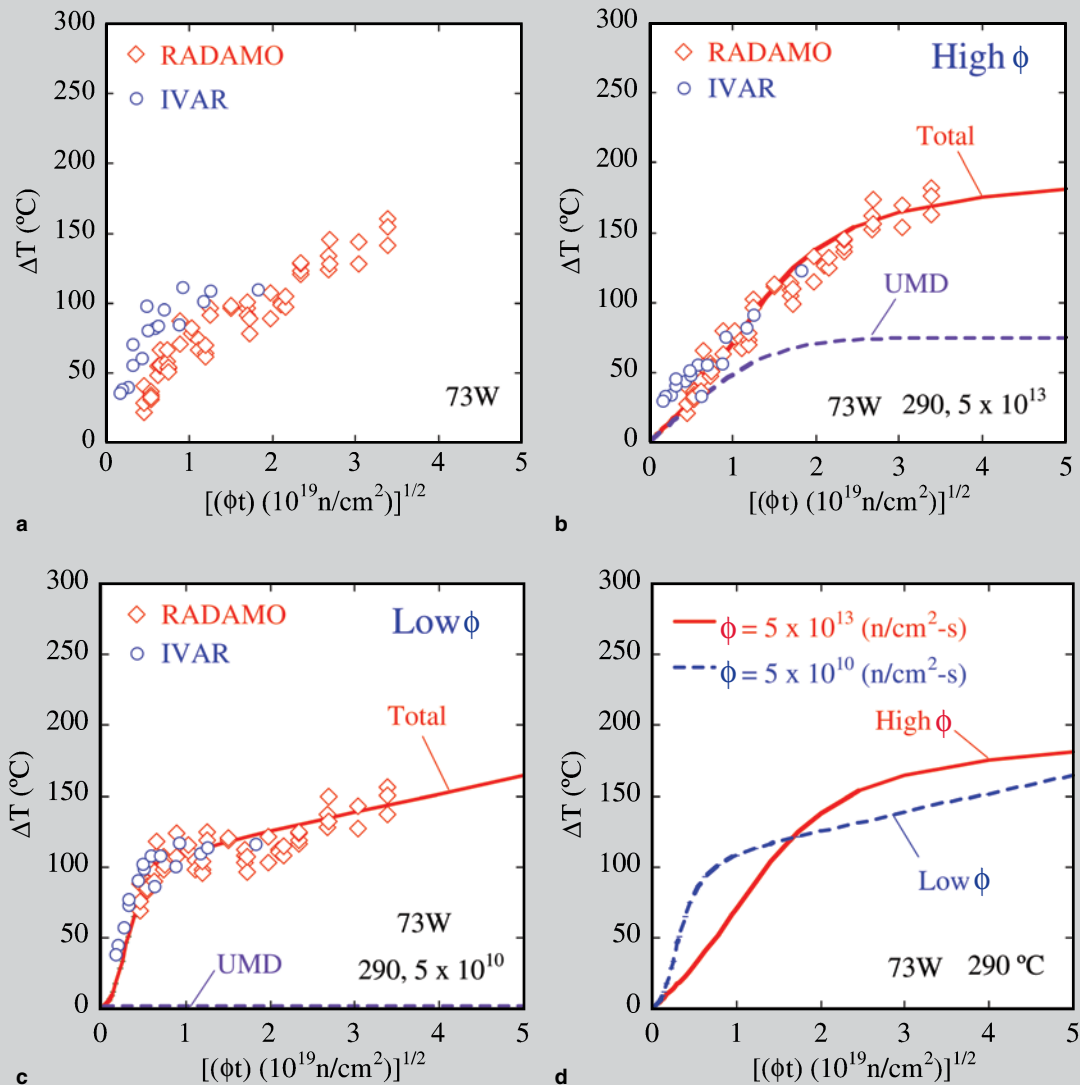


Figure 5. Three feature model ΔT predictions for the high 0.3 wt.% copper weld, 73W: (a) the raw data; (b) predictions for high flux and (c) low flux at 290°C; and (d) comparisons of the high and low flux ΔT curves. The model has been used to adjust the ΔT data to the common irradiation condition specified.

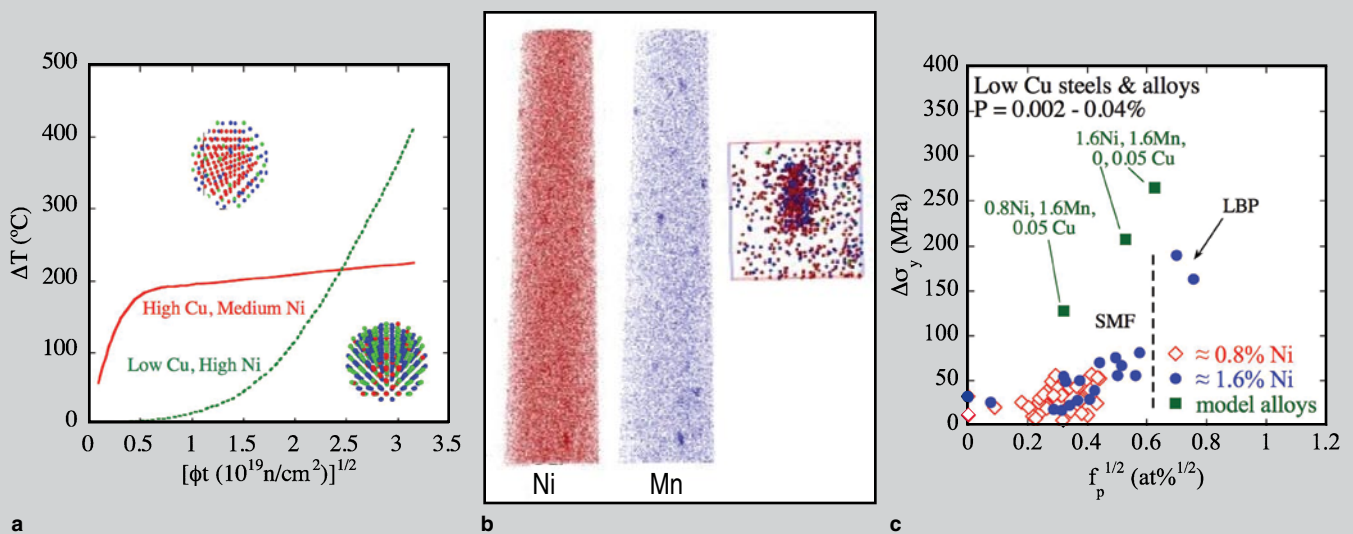


Figure 6. (a) Illustrative model predictions of the fluence dependence of hardening in a high copper, medium nickel steel due to CRP hardening and in high-nickel, low-copper steel due to LBP hardening; (b) APT maps of nickel and manganese distributions and a blowup of an Mn-Ni LBP precipitate in a copper-free 1.6 wt.% Ni-1.6 wt.% Mn model alloy irradiated to 1.8×10^{19} n/cm² at high flux and 290°C; and (c) $\Delta\sigma_y$ as a function of the square root of the volume fraction of precipitates in low copper steels and model alloys.

or higher irradiation temperatures and fluxes. While such hardening is generally attributed to SMF, these results suggest that LBP are actually part of a continuum of chemically complex SMF-LBP features that form in low copper alloys. Thus, the SMF may be precursors to well-defined LBP that subsequently develop at higher fluence. Late-blooming phases and significant $\Delta\sigma_y$ are also found in Mn-Ni-low Cu (≤ 0.05) model alloys irradiated at 290°C and high flux to 1.8×10^{19} (note the model alloys $\Delta\sigma_y(f_p)$ fall above those for complex steels due to strength superposition effects). Higher nickel and trace copper result in larger $\Delta\sigma_y$ in the model alloys, but 0.8% nickel, 1.6% manganese and 0.05% copper are sufficient to produce significant LBP precipitation and hardening.

Thus, it is no longer an issue of if, but rather where and when, LBPs may strike to threaten the continued operation of vulnerable vessels. However, additional research will be required to determine the conditions leading to the formation of LBP, and the severity of the corresponding embrittlement. We also note that other hardening features, especially self-interstitial atom cluster dislocation loops, may be important at high fluence.

CONCLUSIONS

New experimentally verified models must be developed to accurately predict embrittlement, ideally in terms of master toughness-temperature curves, for pertinent low flux, high fluence extended life conditions. Advanced models must also treat potential embrittlement contributions from late blooming phases, as well as ΔT attenuation and following annealing-reirradiation remediation cycles. More specifically:

- New models should resolve issues related to the master curve method; remediation of embrittlement by annealing; currently unmodeled variables and variable combinations; attenuation; and flux effects in the regime pertinent to BWR and PWR surveillance and vessel conditions.
- Improved ΔT models will require combining advanced physical models that are self-consistently

fit to a combination of lower resolution PREDB and pertinent high resolution test reactor data.

- Direct use of high flux test reactor data to predict ΔT for high fluence-low flux conditions may be inappropriate.
- The existence of LBP has been proven. However additional research will be required to determine the detailed conditions leading to the formation of LBP and the severity of the corresponding embrittlement. Other embrittling features may also emerge at high fluence, such as dislocation loops.
- SMF may be precursors to well-defined LBP that subsequently develop at higher fluence, especially at low flux.
- Basic experiments, such as low temperature annealing, are needed to help develop improved physical embrittlement models that account for a very wide range of flux, and that can be used to more reliably predict high fluence-low flux ΔT .
- Progress will require high fluence test reactor irradiations that should be carried out at the lowest feasible flux levels, so as to minimize the need for adjustments.

References

1. E.D. Eason et al., *A Physically Based Correlation of Irradiation-Induced Transition Temperature Shifts for RPV Steels* (Oak Ridge, TN: Oak Ridge National Laboratory, 2007), ORNL/TM-2006/530.
2. G.R. Odette and G.E. Lucas, *JOM*, 53 (7) (2001), p. 18.
3. R.K. Nanstad, M.A. Sokolov, and D.E. McCabe, "Applicability of the Fracture Toughness Master Curve to Irradiated Highly Embrittled Steel and Intergranular Fracture," *J. ASTM Int.*, 5 (3) (2008), Paper ID JA1101346. Available online at www.astm.org.
4. U.S. Nuclear Regulatory Commission, *Radiation Embrittlement of Reactor Vessel Materials, Regulatory Guide 1.99, Revision 2* (Washington, D.C.: U.S. Nuclear Regulatory Commission, 1988).
5. G.R. Odette, *Script. Met.*, 17 (1983), p. 1183.
6. G.R. Odette et al., *The Irradiation Variables (IVAR) Program Database on Irradiation Induced Yield and Ultimate Tensile Stress Changes in Reactor Pressure Vessel Steels*, UCSB MRPG PV1-2009 (Santa Barbara, CA: UES Materials Reliability and Performance Group, UCSB, 2009).
7. G.R. Odette and G.E. Lucas, *Radiation Effects and Defects in Solids*, 144 (1-4) (1998), p. 189.
8. M. EricksonKirk, "A Review of ΔT_{30} Data for Reactor Pressure Vessel Steels Obtained at High Fluences," *J. ASTM Intl.* (West Conshohocken, PA: ASTM Intl., 2009), JA1102000-8.
9. G.R. Odette, *Microstructural Evolution During Irradiation*, MRS Symp. Proc. 373 (Warrendale, PA: Materials Research Society, 1995), p. 137.
10. G.R. Odette, *Irradiation Effects on Pressure Vessel*

11. G.R. Odette and B.D. Wirth, *J. Nucl. Mat.*, 251 (1998), p. 157.
12. G.R. Odette, T. Yamamoto, and B.D. Wirth, *Proceedings of the Second International Conference on Multiscale Modeling* (University of California Los Angeles, 2004), p. 105.
13. M.K. Miller and K.F. Russell, "Embrittlement of RPV Steels: An Atom Probe Tomography Perspective," *J. Nuc. Mat.*, 37 (1-3) (2007), p. 145.
14. M.K. Miller et al., *J. Nuc. Mat.*, 385 (2009), p. 615.
15. J.M. Hyde et al., *20th ASTM International Symposium on Effects of Radiation on Nuclear Materials*, ASTM STP 1405 (West Conshohocken, PA: American Society for Testing and Materials, 2001), p. 262.
16. *ASTM Standard E1921-09a, "Determination of Reference Temperature, T_0 , for Ferritic Steels in the Transition Range,"* Annual Book of ASTM Standards, Vol. 03.01 (West Conshohocken, PA: ASTM International, 2009).
17. W.A. Van Der Sluys et al., "Indexing Fracture Toughness Data, Part 1: Results from the MPC Cooperative Test Program on the Use of Precracked Charpy Specimens for T_0 Determination," WRC Bulletin 486 (New York: Welding Research Council, Inc., November 2003).
18. G.R. Odette, T. Yamamoto, and R.D. Klingensmith, *Phil. Mag.*, 85 (2005), p. 779.
19. G.R. Odette et al., *16th International Symposium on the Effects of Radiation on Materials*, ASTM-STP 1175 (West Conshohocken, PA: American Society for Testing and Materials, 1993), p. 373.
20. E.V. Mader, "Kinetics of Irradiation Embrittlement and the Post-Irradiation Annealing of Nuclear Reactor Pressure Vessel Steels" (Ph.D. Thesis, University of California, Santa Barbara, 1995).
21. R.K. Nanstad et al., *Review of Draft NUREG Report on Technical Basis for Revision of Regulatory Guide 1.99*, ORNL/NRC/LTR-08/03 (Oak Ridge, TN: Oak Ridge National Laboratory, 2008).
22. C.L. Liu et al., *Mater. Sci and Eng. A*, 238 (1998), p. 202.
23. W.J. Phythian and C.A. English, *J. Nuc. Mat.*, 205 (1993), p. 162.
24. J.T. Buswell et al., *J. Nuc. Mat.*, 225 (1995), p. 196.
25. G.R. Odette, *Microstructure Evolution During Irradiation*, MRS Symp. Proc. 439 (Warrendale, PA: Materials Research Society, 1998), p. 457.
26. B.D. Wirth et al., *18th International Symposium on the Effects of Radiation on Materials*, ASTM STP-1325 (West Conshohocken, PA: American Society for Testing and Materials, 1999), p. 102.
27. R.G. Carter et al., *J. Nuc. Mat.*, 298 (2001), p. 211.
28. S.C. Glade et al., *J. Nuc. Mat.*, 351 (2006), p. 27.
29. M.K. Miller et al. *J. Nuc. Mat.*, 361 (2-3) (2007), p. 248.
30. G.R. Odette and C. Cowan, "Use of Combined Electrical Resistivity and Seebeck Coefficient Measurements to Characterize Solute Redistribution Under Irradiation and Thermal Aging," *Proceedings of the 10th International Symposium on Environmental Degradation of Materials in Light Water Reactors* (Houston, TX: National Association of Corrosion Engineers, 2001).
31. J.S. Smith, "Characterization of Irradiation and Thermal Aging Induced Solute Redistributions in Reactor Pressure Vessel Steels Using Combined Electrical Resistivity and Seebeck Coefficients" (M.Sc. Thesis, University of California at Santa Barbara, 2006).

G.R. Odette is with the Department of Mechanical Engineering at the University of California, Santa Barbara, CA 93106; odette@engineering.ucsb.edu; and R.K. Nanstad is with Oak Ridge National Laboratory, Oak Ridge, TN.